

# Investigation of tokamak turbulent avalanches using wave-kinetic formulation in toroidal geometry

Camille Gillot<sup>1,2,†</sup>, Guilhem Dif-Pradalier<sup>1,†</sup>, Xavier Garbet<sup>1</sup>,  
 Olivier Panico<sup>1</sup>, Yanick Sarazin<sup>1</sup>, Robin Varennes<sup>1</sup> and David Zarzoso<sup>3</sup>

<sup>1</sup>IRFM, CEA, F-13108 Saint-Paul-lez-Durance, France

<sup>2</sup>Ecole des Ponts ParisTech, Champs sur Marne, France

<sup>3</sup>PIIM, Aix Marseille Université, CNRS, UMR 7345, Marseille, France

(Received 29 July 2020; revised 15 March 2021; accepted 19 March 2021)

The interplay between toroidal drift-wave turbulence and tokamak profiles is investigated using a wave-kinetic description. The coupled system is used to investigate the interplay between marginally stable toroidal drift-wave turbulence and geodesic acoustic modes (GAMs). The coupled system is found to be unstable. Notably, the most unstable mode corresponds to the resonance between the turbulent wave radial group velocity and the GAM phase velocity. For a low-field-side ballooned drift-wave growth, a background flow shear breaks the symmetry between inwards- and outwards-travelling instabilities. Although this turbulence–GAM coupling may not be the primary driver for avalanches in standard core ion temperature gradient simulations, this mechanism is generic and displays many of the expected features, and should be of interest in several other regimes, which include towards the edge or in the presence of energetic particles.

**Key words:** fusion plasma, plasma confinement, plasma instabilities

## 1. Introduction

The estimation of the quasi-linear fluxes requires proper knowledge of the turbulence spectrum. This is a complex endeavour. The turbulent fluxes require computing the two-point correlation function  $\mathcal{C}_\phi(t_1, t_2, \mathbf{x}_1, \mathbf{x}_2)$  of the potential (Adam, Laval & Pesme 1979)

$$\mathcal{C}_\phi(t_1, t_2, \mathbf{x}_1, \mathbf{x}_2) = \langle \phi(t_1, \mathbf{x}_1) \phi(t_2, \mathbf{x}_2) \rangle_{\text{turb}}. \quad (1.1)$$

This correlation function is then weighted appropriately to express the flux carried at  $(t_1, \mathbf{x}_1)$  by a plasma parcel that was displaced from  $(t_2, \mathbf{x}_2)$ . The average  $\langle \cdot \rangle_{\text{turb}}$  is taken on realisations of the system and on unobserved symmetry directions. The determining equations are very complex and can be impractical for both analytical and numerical work (Farrell & Ioannou 2007; Srinivasan & Young 2012). In the case of tokamak plasmas,

† Email addresses for correspondence: [camille.gillot@polytechnique.org](mailto:camille.gillot@polytechnique.org),  
[guilhem.dif-pradalier@cea.fr](mailto:guilhem.dif-pradalier@cea.fr)

turbulence is populated by drift-wave-like micro-instabilities at a high toroidal mode number, which are driven by kinetic interchange coupling.

Explanations for turbulent saturation often revolve around mode coupling. Nonlinear coupling pours an excess of energy from a turbulent eigenmode to stabler eigenmodes, through modulation by a low wavenumber mode or through scattering with other turbulent modes. In the near-marginal regime, avalanches provide an effective vector for heat transport (Diamond & Hahm 1995; Newman *et al.* 1996): bursts travel through the plasma in an almost ballistic fashion (Sarazin & Ghendrih 1998; Sarazin *et al.* 2010). Such avalanches have been linked to the transition from Bohm to gyroBohm scaling for turbulent transport (Carreras *et al.* 1996; Garbet *et al.* 1999; Lin *et al.* 2002; Candy & Waltz 2003). They are routinely observed in both gradient-driven and flux-driven nonlinear simulations (Beyer *et al.* 2000; Idomura *et al.* 2009; McMillan *et al.* 2009; Görler *et al.* 2011; Dif-Pradalier *et al.* 2017), although the comparison between gradient-driven and flux-driven dynamics is still an open problem (Rath *et al.* 2016). The zonal flow patterns found in those simulations tend to be asymmetric with sometimes strong radial localisation (McMillan *et al.* 2011; Dif-Pradalier *et al.* 2015; Zhu, Zhou & Dodin 2018a; Ivanov *et al.* 2020), which have prompted the nickname of a ‘zonal flow staircase’. Several explanations have been advanced for such avalanches, from self-organised criticality in the sub-marginal regime (Bak, Tang & Wiesenfeld 1987; Hwa & Kardar 1992; Schekochihin, Highcock & Cowley 2012; van Wyk *et al.* 2016; Pringle, McMillan & Teaca 2017; McMillan, Pringle & Teaca 2018), to nonlinear motion of turbulent potential filaments (Beyer *et al.* 2000; Sarazin *et al.* 2010; Gillot 2020). The coupling to the axisymmetric modes and especially zonal flows is of particular interest, because they shear turbulent eddies and act as an efficient means to saturate the turbulence. One of the drivers of the growth of zonal flows is the so-called zonostrophic instability. This instability arises from a modulational coupling of two drift waves, which gives energy to the sheared zonal flow (Champeaux & Diamond 2001; Diamond *et al.* 2005). When turbulent structures and zonal flows act on different radial and temporal scales, individual modulations can be thought of as infinitesimal: the problem can be modelled through the dynamics of a turbulence spectrum alone, forgetting individual wave–wave interactions. This approach has been applied to the modelling of drift waves on the temperature gradient and trapped electron modes, see Anderson *et al.* (2002, 2006), Srinivasan & Young (2012), Parker (2016), Gillot (2016), Ruiz (2017) and Zhu *et al.* (2018b).

Top-of-the-shelf quasi-linear models often rely on a quasi-stationary ansatz to close the turbulence spectrum (Citrin *et al.* 2017). This choice has been criticized as being unable to account for turbulent self-organisation features like zonal flow growth and avalanching for near-marginal turbulence. Wave-kinetic modelling (Weinberg 1962) attempts to estimate the fluctuation spectrum in a simplified manner. The two-point correlations decay with the scale of the turbulent structures. If turbulent structures are much smaller than the background profile scale, the two-point separation can be represented in Fourier space as a local turbulence spectrum  $\mathcal{I}(\mathbf{x}, \mathbf{k})$ . As a result, both the driving gradients and the zonal flows are assumed to be axisymmetric and radially smooth. They should evolve sufficiently slowly for the turbulent structures to adapt adiabatically. In these conditions, an eikonal approach is accessible. By neglecting nonlinear saturation mechanisms, the dynamics can be reduced to a kinetic equation on the spectrum  $\mathcal{I}$ . The so-called wave-kinetic equation is written as

$$\partial_t \mathcal{I} + \partial_{\mathbf{k}} \omega \cdot \partial_{\mathbf{x}} \mathcal{I} - \partial_{\mathbf{x}} \omega \cdot \partial_{\mathbf{k}} \mathcal{I} = 2\gamma \mathcal{I} + \text{Saturation}. \quad (1.2)$$

The saturation term corresponds to nonlinear couplings between turbulent cells and the saturation level they prescribe. In full generality, this term requires higher-order

correlation functions. By analogy with the Boltzmann equation, the saturation term is often approximated by some kind of ‘eddy–eddy’ collision operator (Ruiz, Glinsky & Dodin 2019). Here,  $\omega + i\gamma$  is the eigenmode angular frequency and growth rate, computed from the dispersion relation. The variable  $\mathcal{I}$  represents a conserved wave action. It can be defined using the Wigner density function of the potential, or equivalently the Fourier transform of the two-point correlation function  $\mathcal{C}_\phi$

$$\mathcal{I}(t, \mathbf{x}, \mathbf{k}) = \int \partial_c \mathcal{D} \mathcal{C}_\phi \left( t + \frac{\tau}{2}, t - \frac{\tau}{2}, \mathbf{x} + \frac{\mathbf{s}}{2}, \mathbf{x} - \frac{\mathbf{s}}{2} \right) \exp(i\omega\tau - i\mathbf{k} \cdot \mathbf{s}) \, ds \, d\tau \, d\omega, \quad (1.3)$$

where the function  $\partial_c \mathcal{D}(t, \omega, \mathbf{x}, \mathbf{k})$  will be made explicit later.

Using the time scale separation between the wave frequency and the evolution of background profiles, the wave-kinetic framework models waves as following the local dispersion relation  $\omega = \omega(t, \mathbf{x}, \mathbf{k})$ . As a consequence, (1.3) can be rewritten as

$$\begin{aligned} \mathcal{I}(t, \mathbf{x}, \mathbf{k}) \delta(\omega - \omega(t, \mathbf{x}, \mathbf{k})) &= \partial_c \mathcal{D} \int \mathcal{C}_\phi \left( t + \frac{\tau}{2}, t - \frac{\tau}{2}, \mathbf{x} + \frac{\mathbf{s}}{2}, \mathbf{x} - \frac{\mathbf{s}}{2} \right) \\ &\times \exp(i\omega\tau - i\mathbf{k} \cdot \mathbf{s}) \, ds \, d\tau. \end{aligned} \quad (1.4)$$

The choice of a wave-kinetic formulation in opposition to an eikonal formulation is not without consequences. The nonlinear coupled evolution of the amplitude  $\mathcal{A}_p(t, \mathbf{x})$  and phase  $\sigma_p(t, \mathbf{x})$  of individual wave packets  $\phi_p = \mathcal{A}_p(t, \mathbf{x}) \exp i\sigma_p(t, \mathbf{x})$  is lost, and replaced by a statistical description. One may expect to lose valuable phase information and the associated phase dynamics. Nevertheless, the wave-kinetic approach has been successfully implemented for the drift-wave coupling to zonal flows in Parker (2015, 2016), Gillot (2016), Ruiz *et al.* (2016), Ruiz (2017) and Zhu *et al.* (2018*b*).

In this framework, and in a simplified slab geometry, a seed zonal flow shears the turbulent eddies, which makes the spectrum  $\mathcal{I}$  asymmetric in  $k_r$ . This induces a non-zero Reynolds stress  $\mathcal{R}$ , which reinforces the zonal flow

$$\mathcal{R}(t, \mathbf{x}) = \int \frac{k_r k_\theta}{\mathcal{D}_c} \mathcal{I}(t, \mathbf{x}, \mathbf{k}) \frac{d\mathbf{k}}{(2\pi)^2}. \quad (1.5)$$

As a consequence, the zonal flow grows as  $\gamma \propto k_{r,ZF} \sqrt{\mathcal{E}}$ , with  $\mathcal{E}$  as the turbulent energy, proportional to  $\mathcal{I}$ . This growth rate diverges at high-zonal-flow wavenumber  $k_{r,ZF}$ . Actually, for thinner zonal flows, the free-energy source, which is the density gradient, is modified. The associated diamagnetic drift is sheared in the opposite direction ( $\mathbf{b} \times \nabla n \sim -k_{r,ZF}^2 u_E$ ). The zonal flow growth is stabilised (Parker 2016), with a weaker global growth.

In the case of a tokamak plasma, toroidicity makes everything more complicated. Turbulence has to make do with ballooning and magnetic shear. The radial mode number results from a competition between polarisation, magnetic shear and parallel acoustic dynamics. This severely impacts the shearing effect on the turbulence (Garbet *et al.* 2002) by providing an effective recall towards low-field-side ballooning. This constrains the accessible transverse mode numbers. However, the response of the zonal flows is also modified, as it is coupled to the Landau-damped geodesic acoustic modes (GAMs) (Qiu, Chen & Zonca 2018).

GAMs have been shown to have a mitigating effect on turbulence by various authors (Hallatschek & Biskamp 2001; Waltz & Holland 2008). In addition, simulations with both ion temperature gradient (ITG) and energetic-particle-driven GAMs (EGAMs) feature

increased turbulent avalanches, which are synchronised at the EGAM frequency (Zarzoso *et al.* 2013). Furthermore, the nonlinear interaction of a GAM on an ITG mode can produce another ITG mode through parametric decay (Girardo 2015). The ITG turbulence has a radial group velocity which scales with the magnetic drift. In certain conditions, the slab zonostrophic instability has been shown to have a travelling branch (Ruiz *et al.* 2016). The GAMs have a radial phase velocity that the slab Euler equation does not have, which also scales with the magnetic drift velocity. When the radial motion of turbulent structures matches that of the GAM, the turbulent wave gets trapped inside the GAM (Sasaki 2018; Sasaki *et al.* 2018*b*). The coupled system is unstable and features travelling solutions (Sasaki *et al.* 2016, 2018*a*). These unstable solutions are investigated as candidates for turbulent avalanches.

The wave-kinetic equation is among the simplest models for the evolution of the turbulence spectrum used by the quasi-linear model. We investigate some of the added features of this extended quasi-linear model. In particular, we formulate the coupling between an axisymmetric gyro-kinetic description and a wave-kinetic description of the turbulence spectrum, and investigate whether this model is able to recover some self-organisation features. In particular, we propose to extend the model from Sasaki *et al.* (2018*a*) to the kinetic description of GAMs. Along the way, we derive a self-consistent wave-kinetic equation for any dispersion relation (§ 2), along with its back reaction on the profiles (§ 3). As a consistency check, we apply the formalism to a simple slab drift-wave model (§ 4). We model the laminar profiles using the axisymmetric component of the Vlasov equation, keeping the poloidal dependency to access GAM dynamics. The non-axisymmetric components are modelled using the wave-kinetic equation, using a general dispersion relation for the ITG mode (§§ 5 and 6).

We show that the GAM radial phase velocity and the wave-kinetic radial advection resonate, which destabilises the GAM mode into a radially moving zonostrophic instability. When introducing a population of energetic particles, this resonance happens at the EGAM frequency, and so does the zonostrophic instability. When the turbulence growth rate is poloidally uniform, neither an up-down asymmetry in the turbulence intensity nor a background flow shear are enough to introduce a preferred radial direction for the unstable mode. However, this asymmetry can be triggered by the cooperation between both a background flow shear and a turbulence growth ballooned on the low-field side. The direction of this asymmetry is consistent with the observation from Idomura *et al.* (2009) and McMillan *et al.* (2009): avalanches propagate according to the sign of the background zonal flow shear rate. Although McMillan *et al.* (2009) excludes a GAM-related explanation in the core, because of the mismatch between the GAM frequency and the avalanche burst rate, the presence of energetic particles or an increased temperature gradient towards the edge are able to reverse this ordering. These features make this travelling unstable coupled mode between turbulence and GAMs a candidate explanation for the triggering of turbulent avalanches. The avalanche is then able to travel through the plasma, as shown in Villard *et al.* (2019).

## 2. Derivation of the wave-kinetic equation

The wave-kinetic equation models small-scale waves as pseudo-particles inside the plasma. The waves should maintain their coherence at their scale, and should only be affected by local properties of the background plasma. The pseudo-particles move according to geometrical optics. Their spatial motion is given by their group velocities. In an inhomogeneous or dispersive medium, the waves are distorted and their wavenumber changes.

The wave-kinetic equation has found various applications in plasma physics since its introduction by Weinberg (1962). Its use in turbulence modelling has often relied on *ad hoc* formulations like in Diamond *et al.* (2005) and Sasaki *et al.* (2018a). Conversely, several authors have attempted a simple self-consistent formulation of this model (Dodin & Fisch 2012; Parker 2016; Ruiz 2017), and found earlier versions to be missing essential physics for the saturation of the zonal flows (Parker 2015; Ruiz *et al.* 2016).

We consider in the following a bath of ideal waves, oscillating at high frequency and high wavenumber, in an inhomogeneous medium with slower and smoother evolution. As an extension to the quasi-linear framework, the wave-kinetic equation relies on the same assumptions as the usual quasi-linear computations of the matter and heat fluxes: the temporal scale separation between the wave dynamics and the dynamics of the profiles, and a spatial scale separation between the local description of the ITG mode and of the smoother profiles and zonal flows. In our case, the fastest time scale for the dynamics of the profiles is the GAM, which corresponds to the assumption  $\omega_{\text{turb}} \gg \omega_{\text{GAM}}$ . Because of the scaling  $\omega_{\text{turb}}/\omega_{\text{GAM}} \sim k_{\perp} \rho_i R |\nabla T|/T$ , this separation is marginal in the plasma core, but relevant near the edge with the steeper gradients. The scale separation allows the treatment of the waves as point particles, neglecting their finite correlation length, and their response to profile evolution is instantaneous. However, the radial scale separation may only be marginal, because of the radial pattern of zonal flow staircases (Dif-Pradalier *et al.* 2015; Ivanov *et al.* 2020). The case of non-ideal waves is plagued by numerous technical and fundamental difficulties that we can avoid here by restricting ourselves to the ideal case (Brillouin 1960). This is possible as long as  $\gamma_{\text{turb}} \ll \omega_{\text{GAM}}$ . For plasmas driven close to marginal instability, this is typically the case.

Our derivation follows those in Whitham (1965), Jimenez & Whitham (1976) and Kaufman, Ye & Hui (1987), based on a postulated wave action principle. The idea is to define a variational principle for the waves, and then to derive the wave-kinetic and Poisson equation from it. Using an action principle will allow the self-consistent derivation of the dynamics when the turbulent background is coupled to the evolution of the profiles, while ensuring the correct conservation properties. In the limit of ideal waves, this derivation is equivalent to those by McDonald & Kaufman (1985), McDonald (1988) and Dodin & Fisch (2012), while being algebraically much simpler for resonant instabilities. Local drift-wave modes, such as the ITG, obey a scalar dispersion  $\mathcal{D}(c, r, \zeta)$  in mixed Fourier space for the local ITG modes. Here,  $n$  is the toroidal mode number,  $c = \omega/n$  is the mode angular phase velocity,  $r$  is the reference radial position of the mode and  $\zeta = k_r/nq'$  is its ballooning angle. By symmetry, we assume  $n > 0$ . The eigenfrequency is obtained as a function of  $r$  and  $\zeta$  by solving  $\mathcal{D}(c) = 0$ . In the case of multiple branches, an index can be introduced to lift the ambiguity. We are neglecting growth and damping of the waves. In the kinetic regime, the growth and damping are carried by the imaginary part of  $\mathcal{D}$ . Incidentally, we assume  $\mathcal{D}$  to be real.

As a starting point, we recast the problem as an action principle

$$\mathcal{S} = \int \frac{\mathcal{N} e^2}{2T} \mathcal{D}(c, r, \zeta, n) |\phi|^2 r \, dr n^2 q' \, d\zeta \, dc, \quad (2.1)$$

where  $\mathcal{N}$  is the plasma density,  $T$  is the temperature and  $e$  is the electron charge. With this formulation, the normalisation of  $\mathcal{D}$  has to be chosen with care to ensure the consistency between the first-principle action and this reduced  $\mathcal{S}$ . See § 4 for an example.

Equivalently, the mode dispersion relation is obtained by setting  $\partial \mathcal{S} / \partial |\phi|^2 = 0$ . A scalar dispersion relation  $\mathcal{D}$  is defined up to a function of  $r, \zeta, n$ . The normalisation of the integrand is chosen so as to retrieve the Poisson variational principle in the high

frequency limit.

$$\mathcal{S} \xrightarrow{c \rightarrow \infty} \int \frac{\mathcal{N} e^2}{2T} k_{\perp}^2 \rho_i^2 |\phi|^2 r \, dr n^2 q' \, d\zeta \, dc. \tag{2.2}$$

The wave-kinetic equation describes the behaviour of the amplitude of turbulent waves and abstracts out their precise shape. This argument can be made to be precise by introducing an amplitude–phase decomposition of the potential as a sum of wave-packets  $p$

$$\phi(t, r, \theta, \varphi) = \sum_p \sqrt{\frac{2T \mathcal{A}_p(t, r)}{\mathcal{N} e^2}} \exp(i\sigma_p(t, r, \theta) + i\varphi), \tag{2.3}$$

where  $\mathcal{A}_p$  plays the role of the energy in the fluctuation and  $\sigma_p$  is a real phase function. Here,  $\mathcal{A}_p$  is a very smooth function, while  $\sigma_p$  contains the fine details. To avoid cluttering the notation, the subscript  $p$  will remain implicit except when otherwise noted.

The computations leading to (2.1) can be redone using  $\omega = -\partial_t \sigma$ ,  $k_r = \partial_r \sigma$  instead of the ballooning phase function  $\sigma = -nct - nq(\theta - \zeta)$ , and neglecting the second derivatives of  $\sigma$ . These second derivatives are related to the coherence and finite extent of the waves, and are neglected by construction. Here  $\mathcal{A}$  is assumed to be constant at the scale of the waves, so its derivatives are neglected. This allows the definition of the eikonal action principle as

$$\mathcal{S}_{\text{eik}} = \sum_p \int \mathcal{D} \left( t, c = -\frac{\partial_t \sigma_p}{n}, r, \zeta = \frac{\partial_r \sigma_p}{nq'}, n \right) \mathcal{A}_p(t, r) r \, dr \, dt, \tag{2.4}$$

with the exact same dispersion relation  $\mathcal{D}$ . The variations of  $\mathcal{S}_{\text{eik}}$  with respect to  $\mathcal{A}$  give the dispersion relation (2.5), but applied to derivatives of  $\sigma$ . The wave conservation equation (2.6) corresponds to the variations of  $\mathcal{S}_{\text{eik}}$  with respect to  $\sigma$ .

$$\mathcal{D} \left( t, c = -\frac{\partial_t \sigma}{n}, r, \zeta = \frac{\partial_r \sigma}{nq'}, n \right) = 0 \tag{2.5}$$

$$\partial_t (\mathcal{A} \partial_c \mathcal{D}) - \frac{1}{r} \partial_r \left( r \mathcal{A} \frac{\partial_{\zeta} \mathcal{D}}{q'} \right) = 0. \tag{2.6}$$

These two equations are valid for each wave packet individually. By analogy with traditional mechanics, (2.5) is called the Hamilton–Jacobi equation. In resolved form, it would be written as  $c(x, \partial_r \sigma) = -\partial_t \sigma$  with  $c(x, k)$  as the wave phase velocity from the dispersion relation. The phase function  $\sigma$  serves as a pilot wave. It has a similar role as Hamilton’s function for the motion of the individual turbulent waves: it provides the evolution of the canonical momentum  $k = \partial_x \sigma$  as a function of space and time. Equation (2.6) is already in a conservative form. The convected quantity is  $\mathcal{A} \partial_c \mathcal{D}$ , the ratio of an energy to a toroidal phase velocity. It represents the toroidal momentum stored in the wave packet. We note that the derivative  $\partial_c \mathcal{D}$  must not vanish. This excludes from this description the case of reactive instabilities caused by the encounter of two stable branches. Conversely, this description is adequate for kinetic excited or damped waves, for which  $\partial_c \mathcal{D} \neq 0$ . The system is composed of two nonlinear equations (2.5) and (2.6),

thus is impractical for a bath of wave packets. To derive the wave-kinetic equation, we introduce the Wigner density function (Moyal & Bartlett 1949; McDonald & Kaufman 1985; McDonald 1988, 1991)

$$\begin{aligned} \mathcal{W}(t, r, \zeta) &= \frac{\mathcal{N} e^2}{2T} \int \phi\left(t, r + \frac{x}{2}\right) \phi^*\left(t, r - \frac{x}{2}\right) \exp(-in\zeta q'x) \frac{nq' dx}{2\pi} \\ &\approx \sum_p \mathcal{A}_p \delta\left(\zeta - \frac{\partial_r \sigma_p}{nq'}\right), \end{aligned} \tag{2.7}$$

where  $\delta$  is the Dirac distribution. The second equality is valid thanks to the radial scale separation between  $\mathcal{A}$  and  $\sigma$ . The function  $\mathcal{W}$  encodes both the amplitude and the phase. It serves as a Klimontovitch distribution for the wave packets. Using Whitham’s equation (2.6), the convection of the wave action density  $\mathcal{W}$  can be computed as

$$\partial_t(\mathcal{W}\partial_c \mathcal{D}) - \frac{1}{r} \partial_r \left( r \mathcal{W} \frac{\partial_\zeta \mathcal{D}}{q'} \right) = - \left[ \partial_c \mathcal{D} \frac{\partial_r^2 \sigma}{n} - \partial_\zeta \mathcal{D} \partial_r \left( \frac{\partial_r \sigma}{nq'} \right) \right] \partial_\zeta \mathcal{W}. \tag{2.8}$$

The expression inside the square bracket quantifies how radially neighbouring wave trajectories get pulled apart. It will yield the wave stretching term in the wave-kinetic equation. As  $\sigma$  is real, the growth rate term in  $\partial_t \text{Im} \sigma$  does not appear, which corresponds to the assumed ideal waves with  $\gamma = 0$ . Similarly,  $\partial_r \sigma$  is real, which corresponds to propagating waves (Suchy 1981). To compute the bracket, we differentiate the Hamilton–Jacobi equation (2.5) with respect to  $r$

$$0 = \partial_r \left[ \mathcal{D} \left( c = -\frac{\partial_r \sigma}{n}, r, \zeta = \frac{\partial_r \sigma}{nq'}, n \right) \right] = -\partial_c \mathcal{D} \frac{\partial_r^2 \sigma}{n} + \partial_\zeta \mathcal{D} \partial_r \left( \frac{\partial_r \sigma}{nq'} \right) + \partial_r \mathcal{D} \tag{2.9}$$

$$\partial_t(\mathcal{W}\partial_c \mathcal{D}) - \frac{1}{r} \partial_r \left( r \mathcal{W} \frac{\partial_\zeta \mathcal{D}}{q'} \right) = -\frac{\partial_r \mathcal{D}}{q'} \partial_\zeta \mathcal{W}. \tag{2.10}$$

The parameters of  $\mathcal{D}$  in (2.10) are still the derivatives of  $\sigma$ . To replace mentions of  $\partial_r \sigma$  by  $\zeta$ , we use the absorbing property of the Dirac distribution<sup>1</sup> inside  $\mathcal{W}$ . We get the wave-kinetic equation as

$$\partial_t(\mathcal{W}\partial_c \mathcal{D}) - \frac{1}{r} \partial_r \left( r \mathcal{W} \frac{\partial_\zeta \mathcal{D}}{q'} \right) + \partial_\zeta \left( \mathcal{W} \frac{\partial_r \mathcal{D}}{q'} \right) = 0. \tag{2.11}$$

The value of  $\partial_r \sigma$  is completely defined by the Hamilton–Jacobi equation (2.5) as a function of  $r$  and  $\zeta$ . Here  $\sigma$  is completely eliminated from the description. The equation on  $\mathcal{W}$  can be recast as a conservation for the wave action  $\mathcal{I}$

$$\mathcal{I} = \mathcal{W}\partial_c \mathcal{D} = \frac{\mathcal{N} e^2}{2T} |\phi|^2 \delta \left( \zeta - \frac{\partial_r \sigma}{nq'} \right) \partial_c \mathcal{D} \tag{2.12}$$

$$\partial_t \mathcal{I} + \frac{1}{r} \partial_r (r v_g^r \mathcal{I}) + \partial_\zeta (v_g^\zeta \mathcal{I}) = 0. \tag{2.13}$$

<sup>1</sup>This replacement is only possible on functions  $f$  that directly ‘touch’ the  $\delta$  distribution:  $f(a)\delta(a-b) = f(b)\delta(a-b)$ . If a derivative is present, the expression needs to be shuffled to get it out of the way:  $f(a)\partial_b \delta(a-b) = \partial_b [f(a)\delta(a-b)] = \partial_b [f(b)\delta(a-b)]$ .

The growth rate arises from the solution of the complex analytic dispersion relation (2.5). The group velocity  $v_g^r$  and the wave distortion  $v_g^\zeta$  are given by the usual formulae

$$q'v_g^r = -\frac{\partial_\zeta \mathcal{D}}{\partial_c \mathcal{D}} = \left(\frac{\partial c}{\partial \zeta}\right)_{\mathcal{D}=0} \tag{2.14}$$

$$q'v_g^\zeta = \frac{\partial_r \mathcal{D}}{\partial_c \mathcal{D}} = -\left(\frac{\partial c}{\partial r}\right)_{\mathcal{D}=0} . \tag{2.15}$$

Equation (2.13) is a kinetic equation. The waves are advected in phase space so as to conserve the wave angular phase velocity  $c(r, \zeta)$ . Here  $c(r, \zeta)$  actually serves as a Hamiltonian for the waves.

The turbulent energy can be derived using Noether’s theorem from the eikonal action (3.9), and coincides with the usual definition in dispersive media (Landau & Lifschitz 1984, (61.9))

$$E_{\text{turb}} = \int c\mathcal{I} d\zeta r dr = \int \partial_c[c\mathcal{D}] \frac{\mathcal{N} e^2}{T} |\phi|^2 d\zeta r dr, \tag{2.16}$$

where  $c$  is the real solution to the real part of the dispersion relation (2.5). By removing the function  $\sigma$  from the description, the nonlinear phase dynamics associated with the Hamilton–Jacobi equation (2.5) is lost. Only a linearised version is kept in the form of the advection velocities  $v_g^r$  and  $v_g^\zeta$ .

Dimensionally, the total wave action  $\int \mathcal{I} d\zeta$  from (1.3) is an energy divided by a toroidal angular velocity. It represents the momentum of turbulence when waves are sped-up toroidally. Because of the parallel alignment of the turbulent structures,  $q\mathcal{I}$  serves as a poloidal momentum.

### 3. Coupling to the profile

Equation (2.13) is coupled to the Vlasov equation for the axisymmetric component of the distribution function  $\mathcal{F}$

$$\partial_t \mathcal{F} + \text{div } \mathbf{\Gamma}_{\text{traj}} + \text{div } \mathbf{\Gamma}_{\text{turb}} = \text{Sources} + \text{Collisions}. \tag{3.1}$$

Here  $\mathbf{\Gamma}_{\text{traj}}$  is the flux governed by the advection of  $\mathcal{F}$  by the trajectories of the gyro-centres, while  $\mathbf{\Gamma}_{\text{turb}}$  contains the heat flux coming from the nonlinear coupling of non-axisymmetric fluctuations. The latter flux has components along directions  $r, \theta$  and energy  $E$ . In our wave-centred description,  $\mathbf{\Gamma}_{\text{turb}}$  is approximated as the quasi-linear flux, an integral over the spectrum  $\mathcal{I}$ . The integrands encode the efficiency of turbulent transport depending on the class of particles. These depend on the profiles, their gradients and on the wave phase space. Let the linear response  $f$  of the distribution function to the wave  $\phi$  be written symbolically as

$$\frac{f}{\mathcal{F}} = \Lambda \left[ c = -\frac{\partial_t \sigma}{n}, \zeta = \frac{\partial_r \sigma}{nq'}, n; r, \theta, E, \mu \right] \frac{e\phi}{T}. \tag{3.2}$$

For a drift-kinetic system, the dispersion relation with adiabatic electrons can be written as

$$\mathcal{D}_{\text{adiab}} = \tau + k_\perp^2 \rho_i^2 - \frac{1}{\mathcal{N}} \sum_s \int \Lambda_s \mathcal{F}_s d^3 v, \tag{3.3}$$

with  $\tau = T/T_e$  as the ion to electron temperature ratio and  $k_\perp^2 \rho_i^2$  corresponds to the ion polarisation. The extension to a gyro-kinetic model is straightforward by inserting the



appropriate gyro-averaging. The quasi-linear fluxes of gyro-centres read as follows

$$\begin{aligned} \Gamma_{\text{turb}}^r &= \langle v_E^{r*} f \rangle_{\text{turb}} \\ &= -\text{Re} \sum_{n>0} \frac{inq\phi^*}{rB} \Lambda \frac{e\phi}{T} \mathcal{F} \\ &= -\frac{2\mathcal{F}}{e\mathcal{N}} \text{Re} \sum_{n>0} \int \frac{inq}{rB} \Lambda \frac{\mathcal{I}}{\partial_c \mathcal{D}} d\zeta, \end{aligned} \tag{3.4}$$

$$\Gamma_{\text{turb}}^\theta = \langle v_E^{\theta*} f \rangle_{\text{turb}} = \frac{2\mathcal{F}}{e\mathcal{N}} \text{Re} \sum_{n>0} \int \frac{inq'\zeta}{B} \Lambda \frac{\mathcal{I}}{\partial_c \mathcal{D}} d\zeta, \tag{3.5}$$

where the brackets  $\langle \cdot \rangle_{\text{turb}}$  denote a sum over all the turbulent modes for all  $n$  and  $\zeta$ . The turbulence intensity is inserted using its definition equation (1.3).

It should be noted that the total quasi-linear charge fluxes vanish (both the radial and the poloidal components:  $\sum_s e_s \int \Gamma_{\text{turb},s}^{r,\theta} d^3v$ ). In the case of adiabatic electrons, the ion particle flux is ambipolar. This can be seen by integrating (3.4) and (3.5) on velocity.

$$\begin{aligned} \sum_s e_s \Gamma_{\text{turb},s}^r &= 2 \sum_{n>0} \int \frac{nq}{rB} \text{Im} \left[ \frac{1}{\mathcal{N}} \sum_s \int \mathcal{F}_s \Lambda_s d^3v \right] \frac{\mathcal{I}}{\partial_c \mathcal{D}} d\zeta \\ &= 2 \sum_{n>0} \int \frac{nq}{rB} \text{Im} [\tau + k_\perp^2 \rho_i^2] \frac{\mathcal{I}}{\partial_c \mathcal{D}} d\zeta \\ &= 0. \end{aligned} \tag{3.6}$$

The factor inside the brackets is the total density response. The dispersion relation (3.3) tells us it is purely real. Hence, the total charge flux vanishes. This is unexpected: we should get a polarisation flux carried by the turbulence. This polarisation flux contains the Reynolds stress responsible for the growth of zonal flows (Taylor 1915).

There is actually no issue with (3.4) and (3.5). The vanishing of the polarisation flux is consistent with our ordering on radial derivatives  $\partial_r \ll nq'\zeta$ . Because of this ordering, quantities involving an odd number of derivatives are purely imaginary. Instead, the polarisation flux is frozen in the turbulence and appears as an additional charge density in the Poisson equation. For consistency, we need to adapt the Poisson equation to the eikonal action principle (2.4).

The quasi-linear energy flux (3.7) suffers a similar fate

$$\begin{aligned} \Gamma_{\text{turb}}^E &= -e \langle \dot{\mathbf{X}} \cdot \nabla \phi^* f \rangle_{\text{turb}} \\ &= -\frac{2\mathcal{F}}{e\mathcal{N}} \text{Re} \sum_{n>0} \int i\dot{\mathbf{X}} \cdot \nabla \sigma \Lambda \frac{\mathcal{I}}{\partial_c \mathcal{D}} d\zeta \\ &= \frac{2\mathcal{F}}{e\mathcal{N}} \text{Re} \sum_{n>0} \int inq \left( v_D^\theta - \frac{q'}{q} \zeta v_D^r \right) \Lambda \frac{\mathcal{I}}{\partial_c \mathcal{D}} d\zeta. \end{aligned} \tag{3.7}$$

The total energy flux can be decomposed into the effect of resonant wave-particle interactions and of the non-resonant ponderomotive effect. The former corresponds to the work of the quasi-linear fluxes. We suppose that the modes are marginally stable, so

that the dispersion relation is real. As a consequence, there is no direct energy exchange between the particles and the wave, so the resonant energy flux is zero. The ponderomotive energy flux is related to the gradient of the turbulent intensity  $\mathcal{I}$ . Because of the wave-kinetic ordering on the derivatives  $\nabla|\phi|^2 \ll \phi^*\nabla\phi$ , the ponderomotive contribution vanishes. In terms of energy balance, this corresponds to a Boussinesq approximation on the turbulent energy content, akin to what is done with the gyro-kinetic polarisation (Scott & Smirnov 2010). Summing both effects, we are left with no quasi-linear energy flux  $\Gamma_{\text{turb}}^E = 0$ .

Let  $\Phi$  be the axisymmetric electrostatic potential. This potential is associated with a poloidal zonal flow angular velocity  $u_E = \partial_r\Phi/rB$ . Derivations of a dispersion relation are typically done in the toroidally rotating plasma frame, where the zonal flow vanishes. To move back to the laboratory frame, we introduce the zonal flow as a toroidal Doppler shift

$$\mathcal{D}\left(c = -\frac{\partial_t\sigma}{n}, r, \zeta = \frac{\partial_r\sigma}{nq'}, n; u_E\right) = \mathcal{D}\left(c = -\frac{\partial_t\sigma}{n} + qu_E, r, \zeta = \frac{\partial_r\sigma}{nq'}, n\right). \tag{3.8}$$

The complete action principle becomes

$$\begin{aligned} \mathcal{S} &= \int \mathcal{D}\left(c = -\frac{\partial_t\sigma}{n} + \frac{q\partial_r\Phi}{rB}, r, \zeta = \frac{\partial_r\sigma}{nq'}, n\right) \mathcal{A}(t, r) r dr dt \\ &+ \int \frac{m\mathcal{N}}{2B^2} (\nabla_{\perp}\Phi)^2 r dr dt + \int \frac{\mathcal{N}e^2}{2T_e} (\Phi - \Phi_{\text{FS}})^2 r dr dt \\ &- \int \left(\frac{m}{2}v_{\parallel}^2 + \mu B + e\Phi\right) \mathcal{F} d^3v r dr dt. \end{aligned} \tag{3.9}$$

The first line is our eikonal action. The second line contains the kinetic energy stored inside the zonal flow and the third is the energy of the particles. As usual, the Poisson equation is obtained from the variations of  $\mathcal{S}$  with respect to  $\Phi$ .

$$\begin{aligned} -\text{div}_{\perp}\left(\frac{m\mathcal{N}}{B^2}\nabla_{\perp}\Phi\right) + \frac{\mathcal{N}e^2}{T_e}(\Phi - \Phi_{\text{FS}}) - e \int \mathcal{F} d^3v &= \frac{1}{r}\partial_r\left[r\frac{\partial\mathcal{D}}{\partial(\partial_r\Phi)}\mathcal{A}(t, r)\right] \\ &= \text{div}_r \int \frac{q\mathcal{I}}{rB} d\zeta, \end{aligned} \tag{3.10}$$

where the last equality uses (3.8) and the definition of the wave packet density  $\mathcal{I}$ . Turbulence is affected by the poloidal flow  $u_E$ . Modifying the flow costs energy according to a momentum  $q\mathcal{I}$ . This momentum is equivalent to a polarisation for the  $E \times B$  flow. By redefining the distribution function  $\mathcal{F}$ , this charge could be added to the Vlasov equation as our dearly missed polarisation flux. The final system of equations is composed of (2.13), (3.1) and (3.10). The total energy can be derived using Noether’s theorem

$$E_{\text{tot}} = E_{\text{kin}} + E_{\text{pol}} + E_{\text{turb}} \tag{3.11}$$

$$E_{\text{kin}} = \int \left[\frac{m}{2}v_{\parallel}^2 + \mu B\right] \mathcal{F} d^3v r dr d\theta \tag{3.12}$$

$$E_{\text{pol}} = \int \frac{m\mathcal{N}}{2B^2} |\nabla_{\perp}\Phi|^2 r dr d\theta + \int \frac{\mathcal{N}e^2}{2T_e} (\Phi - \Phi_{\text{FS}})^2 r dr d\theta \tag{3.13}$$

$$E_{\text{turb}} = \int \left[c + q\frac{\partial_r\Phi}{rB}\right] \mathcal{I} d\zeta r dr d\theta. \tag{3.14}$$

Here,  $E_{\text{kin}}$  is the energy stored in kinetic form by the particles,  $E_{\text{pol}}$  is the energy stored in the zonal electric field, mostly as the kinetic energy of the zonal flow  $m\mathcal{N}u_E^2/2$  and  $E_{\text{turb}}$  is the energy stored in the turbulence, essentially in the form of kinetic energy of the turbulent  $E \times B$  velocity, eventually screened by the response of the plasma. The Vlasov equation (3.1) is constructed so as to follow the motion of particles according to the Hamiltonian  $(m/2)v_{\parallel}^2 + \mu B + e\Phi$ . Similarly, the wave-kinetic equation (2.13) is constructed so as to follow  $c + q(\partial_r\Phi/rB)$  along the trajectories in phase space. Both dynamics allow one to verify the energy conservation

$$\frac{dE_{\text{kin}}}{dt} = \int \Gamma_{\text{turb}}^E d^3vr dr d\theta - e \int \partial_t\Phi \mathcal{F} d^3vr dr d\theta \tag{3.15}$$

$$\frac{dE_{\text{pol}}}{dt} = \int \frac{m\mathcal{N}}{B^2} \nabla_{\perp}\Phi \cdot \partial_t\nabla_{\perp}\Phi r dr d\theta + \int \frac{\mathcal{N}e^2}{T_e} (\Phi - \Phi_{\text{FS}}) \partial_t\Phi r dr d\theta \tag{3.16}$$

$$\frac{dE_{\text{turb}}}{dt} = \int q \frac{\partial_r^2\Phi}{rB} \mathcal{I} d\zeta r dr d\theta \tag{3.17}$$

$$\frac{dE_{\text{tot}}}{dt} = \int \Gamma_{\text{turb}}^E d^3vr dr d\theta = 0, \tag{3.18}$$

where we have used the Poisson equation (3.10) multiplied by  $\partial_t\Phi$  to get the simplified last equation. The last equation corresponds to the energy exchange between the waves and the particles. For marginally stable modes, it is trivially zero. The conservation of the poloidal momentum can be computed directly from the Poisson equation (3.10)

$$\begin{aligned} \frac{r^2}{q} m\mathcal{N} \partial_t u_E &= \frac{1}{r} \partial_r \int r v_g^r \mathcal{I} d\zeta - e \frac{r}{q} \int \Gamma_{\text{QL}}^r d^3v \\ &= -\frac{1}{r} \partial_r \int r \mathcal{W} \partial_{\zeta} \mathcal{D} d\zeta, \end{aligned} \tag{3.19}$$

where we have used the definition of the radial group velocity  $v_g^r = -\partial_{\zeta}\mathcal{D}/\partial_c\mathcal{D}$ . The first equality corresponds to the definition of the Reynolds stress as a flux of toroidal momentum, while the second equality allows the relation to the potential spectrum.

#### 4. Drift-wave model

As a pedagogical example, let us first apply our approach of the wave-kinetic equation to the well-known Charney–Hasegawa–Mima model for slab drift-waves (Charney & Drazin 1961; Hasegawa & Mima 1978). The advection equation for the vorticity  $w(x, y)$  has a particularly simple form

$$\partial_t w + \mathbf{v}_E \cdot \nabla w + \beta \partial_y \phi = 0. \tag{4.1}$$

We introduce the amplitude  $\mathcal{A}$  and phase function as in (2.3)

$$\tilde{\phi} = \sqrt{2\mathcal{A}} \exp(i\sigma(t, x) + ik_y y). \tag{4.2}$$

Around a reference radial position  $x$ , with a background flow  $u_E = \partial_x\Phi$  in the  $y$  direction, the linearised response for (4.1) is easily computed as

$$\tilde{w} = \frac{\beta - \partial_x W}{c + u_E} \tilde{\phi}, \tag{4.3}$$

with  $W$  as the equilibrium vorticity profile and  $c = -\partial_t \sigma / k_y$  as the phase velocity in the  $y$  direction. The action principle for the Poisson equation becomes

$$\mathcal{S} = \frac{1}{2} \int [\rho_i^2 |\nabla \phi|^2 + \tau |\phi|^2 - \phi w[\phi]] dx dy dt \tag{4.4}$$

$$= \int \mathcal{D} \left( -\frac{\partial_t \sigma}{k_y} + u_{E,x}, \frac{\partial_x \sigma}{k_y}, k_y \right) \mathcal{A} dx dt \tag{4.5}$$

$$\mathcal{D}(c, r, \zeta, n) = k_y^2 \rho_i^2 (1 + \zeta^2) + \tau - \frac{\beta - \partial_x W}{c} = 0, \tag{4.6}$$

where  $\zeta = \partial_x \sigma / k_y$ . The  $k_y^2 \rho_i^2 (1 + \zeta^2)$  is the Laplacian operator in the Poisson equation. The dispersion relation for the drift waves is  $\mathcal{D}(c, r, \zeta, n) = 0$ . We introduce the Wigner function  $\mathcal{W}$  and the wave action density  $\mathcal{I}$

$$\mathcal{W} = \int \phi(x + \delta x) \phi(x - \delta x) \exp(-in\zeta x) n dx = 2\mathcal{A}\delta \left( \zeta - \frac{\partial_x \sigma}{n} \right) \tag{4.7}$$

$$\mathcal{I} = \mathcal{W} \partial_c \mathcal{D} = \frac{\beta - \partial_x W}{c^2} \mathcal{W} = \frac{(\tau + k_\perp^2 \rho_i^2)^2}{\beta - \partial_x W} \mathcal{W}. \tag{4.8}$$

By following the steps in §§ 2 and 3, the wave-kinetic equation (2.13) and the Poisson equation (3.10) become

$$\partial_t \mathcal{I} - \partial_x \left[ \frac{\partial_\zeta \mathcal{D}}{\partial_c \mathcal{D}} \mathcal{I} \right] + \partial_\zeta \left[ \frac{\partial_x \mathcal{D}}{\partial_c \mathcal{D}} \mathcal{I} \right] = 0 \tag{4.9}$$

$$-\nabla^2 \Phi = \partial_x \int \mathcal{I} d\zeta dn, \tag{4.10}$$

with the group velocities given by

$$v_g^x = -\frac{\partial_\zeta \mathcal{D}}{\partial_c \mathcal{D}} = -2\zeta n^2 \rho_*^2 \frac{\beta - \partial_x W}{[n^2 \rho_*^2 (1 + \zeta^2) + \tau]^2} \tag{4.11}$$

$$v_g^\zeta = \frac{\partial_x \mathcal{D}}{\partial_c \mathcal{D}} = -\frac{\partial c}{\partial x} = -\partial_x u_E + \frac{\partial_x^2 W}{n^2 \rho_*^2 (1 + \zeta^2) + \tau}, \tag{4.12}$$

with  $\rho_* = \rho_i / r$ . The expression of the Reynolds stress is retrieved by considering the time evolution of  $u_E$

$$-\partial_t \partial_x \Phi = \partial_x \int \frac{\partial_\zeta \mathcal{D}}{\partial_c \mathcal{D}} \mathcal{I} d\zeta dn = \partial_x \int \rho_*^2 n^2 \zeta \mathcal{W} d\zeta dn. \tag{4.13}$$

We recover the conservation of the Wigner function of the vorticity and not of the potential. As we are placing ourselves in the limit of quasi-static modulation (dubbed  $\omega_{\text{turb}} \ll \omega_{\text{GAM}}$  above), this is consistent with the observations from the geometrical optics limit of the second cumulant expansion (Gillot 2016; Parker 2016). The formulation of the Reynolds stress exactly matches the expected  $k_x k_y |\phi|^2$  from the Euler equation, with less usual notations. Although derived from a different formalism, the obtained wave-kinetic system with velocity (4.12) features the saturation mechanism highlighted in Parker (2015) and Ruiz *et al.* (2016). Its origin lies in the depletion of the free-energy source  $\partial_x W = -\partial_x^2 u_E$ . The next section extends the physics application to the toroidal ITG mode.

### 5. Generalised ITG model

To avoid notation complexity, we consider a prototype generalised ITG model. The instability mechanism stems from the resonance between the toroidal phase velocity  $c$  of the mode and the toroidal drift  $\Omega_d$  of involved particles. In general,  $\Omega_d$  is an even function of  $\zeta$ . For this reason, we shall take  $\Omega_d = \Omega_{d0} + \Omega_{d1} \cos \zeta$ , with  $\Omega_{d0}$  and  $\Omega_{d1}$  of the order of  $u_{DT}$ . The dispersion relation can be written as

$$D(c, r, \zeta, n) = D\left(\frac{c + qu_E}{\Omega_d(\zeta)}, n\right) = 0. \tag{5.1}$$

Without loss of generality, we suppose there is only one branch of solutions  $\delta_n + i\varepsilon_n$  satisfying  $D(\delta_n + i\varepsilon_n, n) = 0$ . In the converse case, the wave-kinetic system can be replaced by a sum over the branches. In this framework, one has

$$c = \Omega_d(\zeta)(\delta_n + i\varepsilon_n) - qu_E. \tag{5.2}$$

Our derivation has been performed for ideal waves only, which neglects the wave–particle energy exchange. For consistency, we further assume no growth rate  $\varepsilon_n = 0$ . The wave-kinetic equation becomes

$$\left. \begin{aligned} \partial_r \mathcal{I} + \frac{1}{r} \partial_r (rv_g^r \mathcal{I}) + \partial_\zeta (\gamma_E \mathcal{I}) &= 0 \\ v_g^r &= \frac{\partial c}{q' \partial \zeta} = -v_g \sin \zeta \\ v_g^\zeta &= -\frac{\partial c}{q' \partial r} = \frac{(qu_E)'}{q'} = \gamma_E, \end{aligned} \right\} \tag{5.3}$$

where the group velocity  $v_g$  scales with the thermal magnetic drift. As expected, the zonal flow shear  $\gamma_E$  acts on waves by an advection in  $\zeta$  space.

### 6. Effect of toroidicity on the zonostrophic instability

Given these three equations (2.13), (3.1) and (3.10), we can discuss their behaviour around a plasma state  $(\mathcal{F}_{eq}, \mathcal{I}_{eq}, \Phi_{eq})$ . For a small departure in the profiles and turbulence intensity, the coupled second-order system can be analysed linearly.

The wave-kinetic equation contains a radial advection (5.3) that scales with the magnetic drift. In certain conditions, this advection gives a travelling branch to the slab zonostrophic instability. In contrast to the slab model, the profiles in the toroidal case respond according to the GAM dynamics. Therefore, one can expect the GAM radial phase velocity and the wave-kinetic radial advection to resonate, which destabilises the GAM mode.

Moreover, the radial velocity scales like (5.3): the inwards/outwards direction depends on the effective ballooning angle. With a background zonal flow shear, the turbulence spectrum is asymmetric in  $\zeta$ . This effect should allow one to explain the relation between the direction of avalanches and the sign of the zonal shear, as reported in numerical simulations (Idomura *et al.* 2009; McMillan *et al.* 2009). We take the coupled system as

$$\partial_r \mathcal{I} + \frac{1}{r} \partial_r (rv_g^r \mathcal{I}) + \partial_\zeta (\gamma_E \mathcal{I}) = 0, \tag{6.1}$$

$$\partial_t \mathcal{F}(r, \theta, E, \mu) + \frac{v_{||}}{qR} \partial_\theta \mathcal{F} - u_D (\cos \theta \partial_\theta + \sin \theta r \partial_r) \mathcal{F} + \frac{b}{B} \times \nabla \Phi \cdot \nabla \mathcal{F} = -\text{div } \Gamma_{QL}, \tag{6.2}$$

where we denote the magnetic drift angular velocity as

$$u_D = \frac{mv_{\parallel}^2 + \mu B}{eBRr}. \tag{6.3}$$

We chose to neglect the effect of the quasi-linear fluxes in (6.2). These fluxes balance the excitation in the wave-kinetic equation. To keep the energetic consistency, we make this excitation zero.

The coupled system (6.1)–(6.2)–(3.10) does not have any known self-consistent solution for non-zero background flow. Notably, numerical simulations feature radial corrugations of the zonal flow pattern. As a consequence, the application of the wave-kinetic method to those equilibria is not straightforward. More accurate descriptions of these equilibria are still under investigation (Kaw, Singh & Diamond 2001; Gürçan *et al.* 2009; Staebler *et al.* 2013; Garbet *et al.* 2020), both in terms of the general shape of the spectrum and the zonal flow pattern. As a consequence, we avoid choosing such an equilibrium, and will only make use of selected components of the eventual turbulence spectrum at equilibrium.

We perturb the system with a fluctuation of the  $n = 0$  potential  $\tilde{\Phi}$ , with  $p/r$  as the radial mode number. Let  $\omega$  be the mode frequency and  $\omega_{\parallel} = v_{\parallel}/qR$ . For simplicity, we neglect the back-action onto the density and temperature gradients used as free-energy sources for the ITG turbulence. As a consequence, the growth of the mode in the thin corrugation limit – around the eddy size – may be overestimated (Parker 2016). In the Vlasov equation, we neglect the poloidal drifts (magnetic and  $E \times B$ ) compared with the poloidal projection of the parallel velocity. We suppose the equilibrium electric field is purely radial  $\Phi_{\text{eq}}(r)$ . The Poisson equation is obtained from (3.10).

$$-i\omega\tilde{\mathcal{I}} - ip\frac{v_g}{r}\sin\zeta\tilde{\mathcal{I}} + \gamma_E\partial_{\zeta}\tilde{\mathcal{I}} = \frac{p^2}{r^2}\frac{\tilde{\Phi}_0}{B}\partial_{\zeta}\mathcal{I}_{\text{eq}} \tag{6.4}$$

$$-i\omega\tilde{F} + \omega_{\parallel}\partial_{\theta}\tilde{F} - u_D\sin\theta r\partial_r\tilde{F} = -[\omega_{\parallel}\partial_{\theta} - u_D\sin\theta r\partial_r]\tilde{\Phi}\frac{\mathcal{F}_{\text{eq}}e}{T_{\text{eq}}} \tag{6.5}$$

$$(-p^2\rho_*^2 + \rho_*^2\partial_{\theta}^2 + \tau)\frac{\mathcal{N}_{\text{eq}}e^2}{T_{\text{eq}}}\tilde{\Phi} = e\int\tilde{F} + ip\int\frac{q\tilde{\mathcal{I}}}{r^2B}d\zeta, \tag{6.6}$$

where we use the local normalised Larmor radius  $\rho_* = \rho_i/r$ . We denote as  $\Phi_{0,c,s}$  the symmetric, cosine and sine components of  $\tilde{\Phi}$ , likewise for  $\tilde{F}$ . We perform a similar decomposition for  $\tilde{\mathcal{I}}$  with the ballooning angle  $\zeta$ .

$$\begin{pmatrix} -2i\omega & -ip\frac{v_g}{r} & 0 \\ -ip\frac{v_g}{r} & -i\omega & -\gamma_E \\ 0 & +\gamma_E & -i\omega \end{pmatrix} \begin{pmatrix} \tilde{\mathcal{I}}_0 \\ \tilde{\mathcal{I}}_s \\ \tilde{\mathcal{I}}_c \end{pmatrix} = \frac{p^2}{r^2}\frac{\tilde{\Phi}_0}{B} \begin{pmatrix} 0 \\ -\mathcal{I}_{\text{eq},c} \\ \mathcal{I}_{\text{eq},s} \end{pmatrix} \tag{6.7}$$

$$\begin{pmatrix} -2i\omega & -ipu_D & 0 \\ -ipu_D & -i\omega & -\omega_{\parallel} \\ 0 & +\omega_{\parallel} & -i\omega \end{pmatrix} \begin{pmatrix} \tilde{F}_0 \\ \tilde{F}_s \\ \tilde{F}_c \end{pmatrix} = \frac{\mathcal{F}_{\text{eq}}e}{T_{\text{eq}}} \begin{pmatrix} 0 & ipu_D & 0 \\ ipu_D & 0 & -\omega_{\parallel} \\ 0 & +\omega_{\parallel} & 0 \end{pmatrix} \begin{pmatrix} \tilde{\Phi}_0 \\ \tilde{\Phi}_s \\ \tilde{\Phi}_c \end{pmatrix} \tag{6.8}$$

We can verify that the matrices on the left-hand side are skew-symmetric. This is consistent with the advection form of the Vlasov and wave-kinetic equations. For simplicity, we set the wave group velocity as  $v_g = u_{\text{DT}}/q'$ , with the thermal toroidal

magnetic drift frequency  $u_{DT} = qT/eBRr$ . Let  $u_{TR}$  be the poloidal transit frequency,  $u_{TR} = v_{th}/qR$ . We introduce the normalised mode frequency  $\Omega = \omega/u_{TR}\sqrt{2}$ , mode number  $P = (u_{DT}/2u_{TR}q)p = q\rho_*p/2$  and background flow shear  $S = (\gamma_E/u_{TR})\sqrt{2}$ . Inverting the two matrices gives the resolved form

$$\tilde{I}_0 = \frac{iP^3/s}{\Omega^2 - S^2 - P^2/s^2} \left[ \mathcal{I}_{eq,c} - i\frac{S}{\Omega}\mathcal{I}_{eq,s} \right] \frac{2\tilde{\Phi}_0}{q^2\rho_*^2r^2u_{TR}B} \tag{6.9}$$

$$\tilde{F}_0 = \frac{e\mathcal{F}_{eq}}{2T_{eq}} \frac{-\Omega P\sqrt{2}\frac{qu_D}{u_{DT}}\tilde{\Phi}_s + 2P^2\left(\frac{qu_D}{u_{DT}}\right)^2\tilde{\Phi}_0}{\Omega^2 - \Omega_{||}^2} \tag{6.10}$$

$$\tilde{F}_s = \frac{e\mathcal{F}_{eq}}{T_{eq}} \frac{-\sqrt{2}\Omega P\frac{qu_D}{u_{DT}}\tilde{\Phi}_0 + \Omega_{||}^2\tilde{\Phi}_s + i\Omega\Omega_{||}\tilde{\Phi}_c}{\Omega^2 - \Omega_{||}^2}, \tag{6.11}$$

with  $s = rq'/q$  as the magnetic shear. For a symmetric distribution function, only the even terms in  $\Omega_{||}$  contribute, so  $\tilde{\Phi}_c$  disappears from the description. Integrating on velocity, we obtain

$$\tilde{N}_0 = \frac{e\mathcal{N}_{eq}}{2T_{eq}} [PI_1\tilde{\Phi}_s + P^2I_2\tilde{\Phi}_0], \tag{6.12}$$

$$\tilde{N}_s = \frac{e\mathcal{N}_{eq}}{T_{eq}} [PI_1\tilde{\Phi}_0 + I_3\tilde{\Phi}_s], \tag{6.13}$$

where we used the resonant integrals from Girardo (2015)

$$I_1 = \sqrt{2} \int \frac{\Omega\frac{qu_D}{u_{DT}}}{\Omega^2 - \Omega_{||}^2} \frac{\mathcal{F}_{eq}}{\mathcal{N}_{eq}} = -\sqrt{2} \left[ Z[\Omega] \left( \frac{1}{2} + \Omega^2 \right) + \Omega \right] \tag{6.14}$$

$$I_2 = 2 \int \frac{\left(\frac{qu_D}{u_{DT}}\right)^2}{\Omega^2 - \Omega_{||}^2} \frac{\mathcal{F}_{eq}}{\mathcal{N}_{eq}} = -2 \left[ Z[\Omega] \left( \frac{1}{2\Omega} + \Omega + \Omega^3 \right) + \frac{3}{2} + \Omega^2 \right] \tag{6.15}$$

$$I_3 = \int \frac{\Omega_{||}^2}{\Omega^2 - \Omega_{||}^2} \frac{\mathcal{F}_{eq}}{\mathcal{N}_{eq}} = -1 - \Omega Z[\Omega], \tag{6.16}$$

with  $Z$  as the Fried and Conte function. Finally, the Poisson equation gives

$$\begin{aligned} \frac{P^2}{q^2}\tilde{\Phi}_0 &= \frac{1}{2}[PI_1\tilde{\Phi}_s + P^2I_2\tilde{\Phi}_0] + i\frac{2P}{r^2\rho_*B}\frac{T_{eq}}{\mathcal{N}_{eq}e^2}\tilde{I}_0 \\ &= \frac{1}{2}[PI_1\tilde{\Phi}_s + P^2I_2\tilde{\Phi}_0] \\ &\quad - 4\tilde{\Phi}_0\frac{P^4/s}{\Omega^2 - S^2 - P^2/s^2} \int \frac{\mathcal{I}_{eq,c} - i\frac{S}{\Omega}\mathcal{I}_{eq,s}}{\mathcal{N}_{eq}mr^2u_{DT}} d\zeta. \end{aligned} \tag{6.17}$$

$$\left( \tau + \rho_*^2 + \frac{P^2}{q^2} \right) \tilde{\Phi}_s = PI_1\tilde{\Phi}_0 + I_3\tilde{\Phi}_s. \tag{6.18}$$

We introduce the turbulence intensity as  $\mathcal{T}_{c,s} = \int \mathcal{I}_{\text{eq},c,s} d\zeta / \mathcal{N}_{\text{eq}} m r^2 u_{\text{DT}}$ . The dispersion relation is given by  $D_G(\Omega) = 0$  with

$$D_G(\Omega) = \frac{1}{q^2} - \frac{J_2(\Omega)}{2} - \frac{I_1^2(\Omega)}{2\left(\tau + \frac{P^2}{q^2} - I_3(\Omega)\right)} \quad (6.19)$$

$$J_2 = I_2 - \frac{8P^2/s}{\Omega^2 - S^2 - P^2/s^2} \left[ \mathcal{T}_c - i \frac{S}{\Omega} \mathcal{T}_s \right]. \quad (6.20)$$

The dispersion function (6.19) is plotted in figure 1. This plot is done with  $q = 1.6$  and  $s = 1$  without any sheared flow  $S = 0$ . The turbulence intensity is chosen as  $\mathcal{T}_c = 10^{-2}$  and  $\mathcal{T}_s = 0$ . This corresponds to an in-out asymmetry of turbulent energy of the order of  $\mathcal{T}_c q^2 \rho_*^2 \varepsilon^2$  times the plasma pressure. For  $P = 0$ , we recover the usual GAM dispersion relation, with  $J_2$  becoming  $I_2$

$$D_{\text{GAM}}(\Omega, P, \mathcal{T}) = \frac{1}{q^2} - \frac{I_2}{2} - \frac{I_1^2}{2\left(\tau + \frac{P^2}{q^2} - I_3\right)}. \quad (6.21)$$

The GAM is located at  $\Omega_{\text{GAM}} = 3.1 - 0.02i$ . For  $P/s$  far from  $\Omega_{\text{GAM}}$ , the zero arising from the zonostrophic instability provides an unstable mode with growth rate  $\Gamma = 0.01$ , and is located near the resonance position  $\Omega = P/s$ . For  $P = 3$ , the two zeros interact. The zonostrophic instability is further destabilised at  $\Omega = 2.8 + 0.35i$ , while the GAM is strongly damped at  $\Omega = 2.8 - 0.38i$ . This example does not contain a linear growth rate for the turbulent structures, so the growth of the zonal flow comes from the pumping energy from turbulence.

It is straightforward to extend the relation dispersion (6.19) to handle EGAMs (Girardo 2015). The same plot can be done with a population of 7% of energetic particles going at 2.8 times the thermal velocity, figure 2. The EGAM lies at  $\Omega = 2.5 + 0.07i$ . For  $P = 2.5$ , the zonostrophic instability interacts with the EGAM. The EGAM is stabilised at  $\Omega = 2.4 - 0.17i$ , while the zonostrophic mode is destabilised to  $\Omega = 2.3 + 0.24i$ . This behaviour is consistent with the observations from Zarzoso *et al.* (2013): the avalanche synchronises at the EGAM frequency when energetic particles are present.

The coupled instability develops at a resonance between the GAM frequency and the turbulent radial group velocity. The resonant radial wavenumber  $k_r$  is a few times  $s/q^2 \rho_i$ . For weak magnetic shear,  $k_r \rho_i$  is a fraction of a unit. The ordering assumption on the radial wavenumber is not ensured. Such inconsistency is typical of the wave-kinetic model (Parker 2016). In addition, the quasi-linear framework, on which wave-kinetic theory is based, is known for its relevance well beyond its validity limits (Laval, Pesme & Adam 2018).

We emphasize that the unstable mode in figures 1 and 2 is not the GAM, but rather the zonostrophic mode which has been pushed-up by the GAM (although the converse can actually happen for EGAMs depending on the plasma parameters Girardo *et al.* 2014). Furthermore, being a resonance process, the destabilisation by the GAM weakens when the GAM damping increases. For GAMs with a sufficiently high damping rate, this mechanism may not operate at all. Similarly, when the damping rate of the GAM depends on the radial position, the dynamics could select the most unstable growth rate for an enlarged radial span, and ensure an undamaged propagation through nonlinear effects. Therefore, we interpret the results from Villard *et al.* (2019) as a destabilisation of our



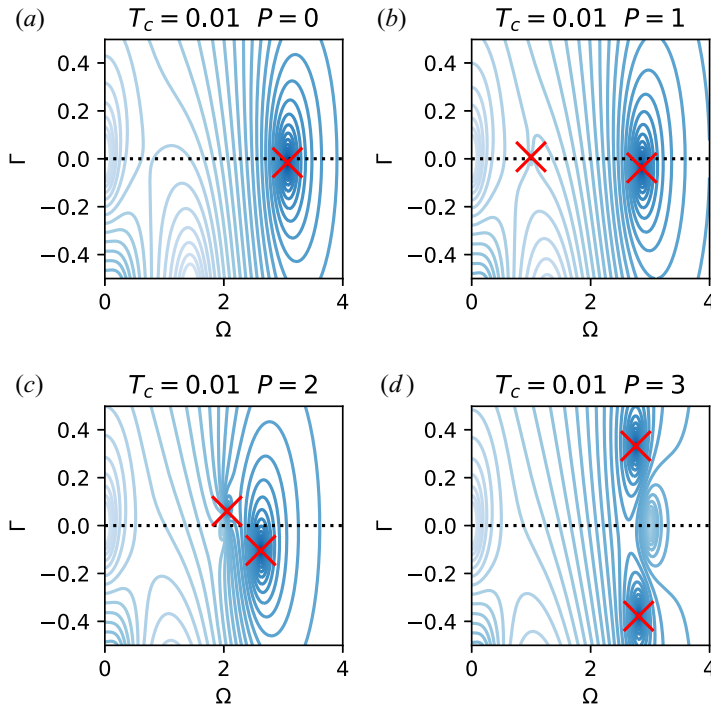


FIGURE 1. Contour lines of  $|D_G|$  for  $q = 1.6$ ,  $\tau = 1$  and  $s = 1$ . Here  $S = 0$ . The GAM frequency is  $\Omega = 3.07 - 0.02i$ . The zeros are in dark blue. The zeros arising from the zonal instability are highlighted by red crosses.

unstable mode close to the edge, at the edge GAM frequency. This mode would propagate inwards from the edge, keeping this edge GAM frequency.

In contrast to the slab drift-wave problem, the unstable modes featured in the dispersion relation (6.19) have bounded growth rates, even for high wavenumbers. This can be shown easily by considering the limit of large growth rate as

$$D_G(\Omega \rightarrow \infty) \approx \frac{1}{q^2} - \frac{J_2(\Omega)}{2} - \frac{1}{\Omega^2 \tau + \Omega^2 \frac{P^2}{q^2} - 1/2} \tag{6.22}$$

$$J_2(\Omega \rightarrow \infty) \approx \frac{2}{\Omega^2} - \frac{8P^2/s}{\Omega^2 - P^2/s^2} \left[ T_c - i \frac{S}{\Omega} T_s \right]. \tag{6.23}$$

Solving this dispersion relation reduces to the roots of the following quartic equation

$$\Omega^4 P^2 s^2 - \Omega^2 (P^4 + P^2 q^2 s^2 + 4P^4 q^2 T_c + q^4 s^2) + P^4 q^2 + P^2 q^4 = 0, \tag{6.24}$$

which has four real roots for  $P$  that are sufficiently large. As a consequence, the approximation of static free-energy sources is acceptable, even in the thin-corrugation limit. This contrasts with the situation of slab drift-waves, where Parker (2016) found this approximation leads to unphysical results.

If we add a non-zero background zonal shear, we expect the system to develop an asymmetry depending on the sign of  $\Omega$ . This is not the case without a turbulent growth rate. Turbulent structures are allowed to travel the full poloidal plane. The system is symmetric in phase velocity, and does not prefer a direction over another. This is a

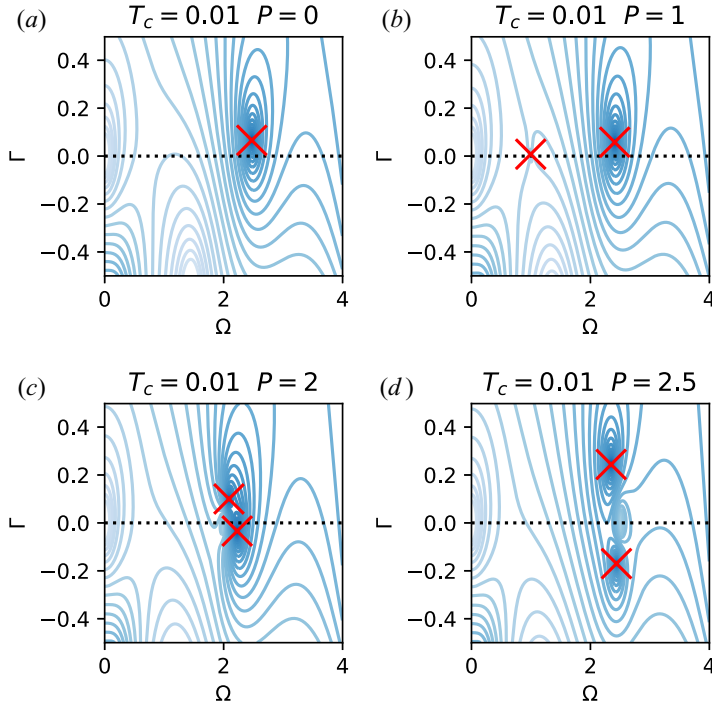


FIGURE 2. Contour lines of  $|D_G|$  for  $q = 1.6$ ,  $\tau = 1$  and  $s = 1$  with 7% energetic particles at 2.8 times the thermal velocity. Here  $S = 0$ . The EGAM frequency is  $\Omega = 2.47 + 0.07i$ . The zeros are in dark blue. The zeros arising from the zonostrophic instability are highlighted by red crosses.

consequence of the joint symmetry principle (Hwa & Kardar 1992; Diamond & Hahn 1995). To regain the asymmetry, we need to take into account the differential growth between the two sides. The damping on the high-field side cuts the poloidal travel of the turbulent structures. We add a growth rate  $\gamma = \alpha \cos \zeta$  to (6.1). The  $\alpha$  coefficient constrains a localised growth of the turbulence on the low-field-side. This effectively expresses the intensity growth where the instability growth is maximum. The  $J_2$  function becomes

$$J_2 = I_2 - \frac{P^2/s}{\Omega^2 + 2A^2 - S^2 - P^2/s^2} \left[ \left( 1 - \frac{AS}{\Omega P} \right) \mathcal{T}_c - i \left( \frac{S}{\Omega} - \frac{A}{P} \right) \mathcal{T}_s \right], \quad (6.25)$$

where  $A = \alpha/u_{TR}$ . By introducing  $A \neq 0$ , the structures are damped when arriving at the high-field side. The symmetry between  $\zeta > 0$  and  $\zeta < 0$  is broken, and the instability can develop with a preferred direction. We consider this modified system with  $A = S = 2$ . The dispersion relation for  $P = 3$  is shown in figure 3. The two instabilities are located at  $\Omega = -2.3 + 0.41i$  and  $\Omega = 2.3 + 0.11i$ . The direction is consistent with the observed inwards avalanches for positive zonal flow shear. In contrast to Sasaki *et al.* (2018a), we do not need to introduce an *ad hoc* up-down asymmetry of the turbulence spectrum, as it is generated self-consistently by the ballooned growth rate and the background flow shear. Nevertheless, such an asymmetry should be expected for tokamaks with realistic magnetic geometry, which would modify the directionality of avalanches as emphasised in Hager & Hallatschek (2012). Although the wave-particle energy exchange is not self-consistent

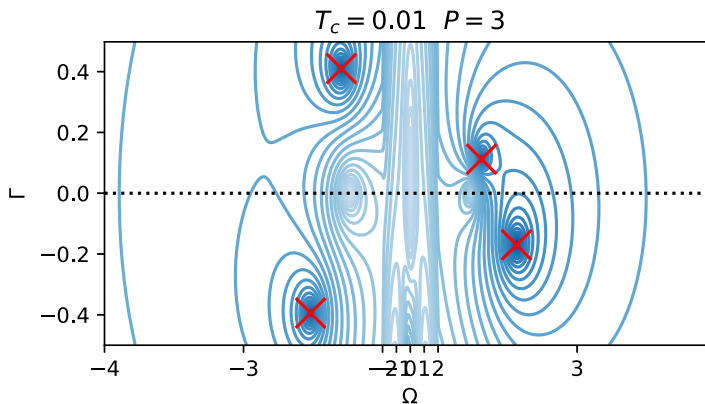


FIGURE 3. Contour lines of  $|D_G|$  for  $q = 1.6$ ,  $\tau = 1$  and  $s = 1$ . Here  $A = S = 2$ . The unstable inwards mode  $\Omega < 0$  is more unstable than the outwards mode. The  $-2 < \Omega < 2$  region has been compressed to help visualisation in the  $2 < |\Omega| < 4$  regions.

for  $\alpha \neq 0$ , the instability mechanism already exists in the self-consistent  $\alpha = 0$  case. As a result, the computed instability is not spurious, but a modification of the former case.

## 7. Conclusion

To study the zonostrophic instability in toroidal plasmas, we developed a self-consistent and conservative formulation of the wave-kinetic equation coupled to a background plasma. This formulation is parameterised by the dispersion relation for the underlying turbulent linear wave, but is restricted to marginally stable modes. It is usable both in slab and toroidal geometry. This conservative formulation has been used to investigate the effect of toroidal geometry on the generation of zonal flows.

In toroidal geometry, zonal flows affect turbulent cells by moving them toroidally and by shearing them. This shearing acts by moving the turbulent cells in the poloidal direction, which make them balloon above or below the mid-plane. As the toroidal drift velocity depends on the ballooning angle of turbulence, the ITG mode frequency follows the same dependency. Because the ballooning angle is related to the radial mode number of the turbulent cell, this induces a radial group velocity of the turbulent cells, which mostly follows the ion direction.

The generic zonostrophic instability carries over from the slab to toroidal geometry. It is driven by the modulation of the drift-wave turbulence by a sheared zonal flow. This generic instability has its phase velocity close to the radial group velocity of the underlying turbulence. In toroidal geometry, the zonal flow responds according to the GAM dynamics, with a specific radial phase velocity. When the radial motion of turbulent cells resonates with the GAM radial phase velocity, the zonostrophic instability and the GAM interact. The zonostrophic instability is further destabilised and the GAM has stronger damping. This mechanism could be responsible for the avalanche behaviour. This is able to reproduce the synchronisation to the EGAM frequency (Zaroso *et al.* 2013). Furthermore, it is able to explain the typical frequency of avalanches, which is close to the GAM frequency in the edge. In the plasma core, the avalanche burst rate is lower than the local GAM frequency. The proposed mechanism should be extended to account for the self-sustainability of avalanches towards the core, and their eventual excitation by lower-frequency modes of the profile.

When a background zonal flow shear is present, a ballooned turbulence has an up-down asymmetry. The footprint of this asymmetry gets carried over to the avalanches by them preferring the same propagation direction. Additional sources of asymmetry are to be expected in more realistic magnetic configurations (Hager & Hallatschek 2012).

The resulting coupled instability develops at a resonance between the GAM frequency and the radial magnetic drift. As a consequence, the resonant radial wavenumber  $k_r$  is a few times  $s/q^2 \rho_i$ . In the weak magnetic shear regime,  $k_r \rho_i$  is a fraction of a unit. As a consequence, the radial scale separation between turbulence and GAMs is only marginally verified. Such inconsistency between the derivation and the application is typical of the wave-kinetic model (Parker 2016). Slower branches of GAMs, like trapped particles driven and precession driven (Sasaki *et al.* 2016), may provide a more reasonable radial scale.

The nonlinear regime with an established GAM has been described by Sasaki (2018) and Sasaki *et al.* (2018*a,b*). An extreme in the flow can act as a trap in phase space for turbulent cells. The toroidal drift-wave phase velocity can be approximated as

$$c \approx -qu_E + \delta_n \Omega_d(\zeta) \approx c_0 - \frac{1}{2}(qu_E)''(r - r_0)^2 - \delta_n \Omega_d(\zeta) \frac{\zeta^2}{2}. \quad (7.1)$$

For maxima of the flow,  $(qu_E)'' > 0$ , the phase velocity is a potential well and turbulent structures may become trapped. On the contrary, for minima of the flow,  $(qu_E)'' < 0$ , the phase velocity has a saddle point and turbulent structures are expelled. This asymmetry has been observed in numerical simulations for gyro-kinetic toroidal systems (McMillan *et al.* 2011; Dif-Pradalier *et al.* 2015; Zhu *et al.* 2018*b*; Gillot 2020; Ivanov *et al.* 2020). The same generic mechanism exists for a stationary zonal flow (Zhu, Zhou & Dodin 2020): the stability of the zonal flow pattern depends on the sign of the curvature. The formalism developed in this article could be extended to account for these additional phenomena.

These trapped eikonal waves actually correspond to stationary radially-coherent waves inside the trap (McDonald 1988). Lifting the eikonal hypothesis may provide useful insight into the nature of nonlinear cooperative structures between GAMs and turbulence.

### Acknowledgements

The authors want to thank Ph. Ghendrih, V. Grandgirard, Ch. Passeron, and acknowledge stimulating discussions with the participants at the 2019 Festival de Théorie in Aix-en-Provence.

*Editor Alex Schekochihin thanks the referees for their advice in evaluating this article.*

### Funding

This work has been carried out within the framework of the EUROfusion Consortium and was supported by the EUROfusion - Theory and Advanced Simulation Coordination (E-TASC) initiative under the TSVV (Theory, Simulation, Verification and Validation) ‘L-H transition and pedestal physics’ project (2019–2020). It has also received funding from the Euratom research and training program. The authors gratefully acknowledge funding from the European Commission Horizon 2020 research and innovation program under Grant Agreement No. 824158 (EoCoE-II). The views and opinions expressed herein do not necessarily reflect those of the European Commission. This work was also granted access to the high-performance computing resources of TGCC and CINES made by GENCI, and to the EUROfusion High Performance Computer Marconi-Fusion.

We acknowledge PRACE for awarding us access to Joliot-Curie at GENCI@CEA, France and MareNostrum at Barcelona Supercomputing Center (BSC), Spain.

## Declaration of interests

The authors report no conflict of interest.

## REFERENCES

- ADAM, J. C., LAVAL, G. & PESME, D. 1979 Reconsideration of quasilinear theory. *Phys. Rev. Lett.* **43** (22), 1671–1675.
- ANDERSON, J., NORDMAN, H., SINGH, R. & WEILAND, J. 2002 Zonal flow generation in ion temperature gradient mode turbulence. *Phys. Plasmas* **9** (11), 4500–4506.
- ANDERSON, J., NORDMAN, H., SINGH, R. & WEILAND, J. 2006 Zonal flow generation in collisionless trapped electron mode turbulence. *Plasma Phys. Control. Fusion* **48** (5), 651–661.
- BAK, P., TANG, C. & WIESENFELD, K. 1987 Self-organized criticality: an explanation of the 1/f noise. *Phys. Rev. Lett.* **59** (4), 381–384.
- BEYER, P., BENKADDA, S., GARBET, X. & DIAMOND, P. H. 2000 Nondiffusive transport in tokamaks: three-dimensional structure of bursts and the role of zonal flows. *Phys. Rev. Lett.* **85** (23), 4892–4895.
- BRILLOUIN, L. 1960 *Wave Propagation and Group Velocity*. Academic Press.
- CANDY, J. & WALTZ, R. E. 2003 Anomalous transport scaling in the DIII-D tokamak matched by supercomputer simulation. *Phys. Rev. Lett.* **91** (4).
- CARRERAS, B. A., HIDALGO, C., SÁNCHEZ, E., PEDROSA, M. A., BALBIN, R., GARCIA-CORTÉS, I., VAN MILLIGEN, B., NEWMAN, D. E. & LYNCH, V. E. 1996 Fluctuation-induced flux at the plasma edge in toroidal devices. *Phys. Plasmas* **3** (7), 2664–2672.
- CHAMPEAUX, S. & DIAMOND, P. H. 2001 Streamer and zonal flow generation from envelope modulations in drift wave turbulence. *Phys. Lett. A* **288** (3–4), 214–219.
- CHARNEY, J. G. & DRAZIN, P. G. 1961 Propagation of planetary-scale disturbances from the lower into the upper atmosphere. *J. Geophys. Res.* **66** (1), 83–109.
- CITRIN, J., BOURDELLE, C., CASSON, F. J., ANGIANI, C., BONANOMI, N., CAMENEN, Y., GARBET, X., GARZOTTI, L., GÖRLER, T., GÜRCAN, O., *et al.* 2017 Tractable flux-driven temperature, density, and rotation profile evolution with the quasilinear gyrokinetic transport model QuaLiKiz. *Plasma Phys. Control. Fusion* **59** (12), 124005.
- DIAMOND, P. H. & HAHM, T. S. 1995 On the dynamics of turbulent transport near marginal stability. *Phys. Plasmas* **2** (10), 3640–3649.
- DIAMOND, P. H., ITOH, S.-I., ITOH, K. & HAHM, T. S. 2005 Zonal flows in plasma—a review. *Plasma Phys. Control. Fusion* **47** (5), 35–161.
- DIF-PRADALIER, G., HORNING, G., GARBET, X., GHENDRIH, P., GRANDGIRARD, V., LATU, G. & SARAZIN, Y. 2017 The  $E \times B$  staircase of magnetised plasmas. *Nucl. Fusion* **57** (6), 066026.
- DIF-PRADALIER, G., HORNING, G., GHENDRIH, P., SARAZIN, Y., CLAIRET, F., VERMARE, L., DIAMOND, P. H., ABITEBOUL, J., CARTIER-MICHAUD, T., EHRLACHER, C., *et al.* 2015 Finding the elusive  $E \times B$  staircase in magnetized plasmas. *Phys. Rev. Lett.* **114** (8).
- DODIN, I. Y. & FISCH, N. J. 2012 Adiabatic nonlinear waves with trapped particles. I. General formalism. *Phys. Plasmas* **19** (1), 012102.
- FARRELL, B. F. & IOANNOU, P. J. 2007 Structure and spacing of jets in barotropic turbulence. *J. Atmos. Sci.* **64** (10), 3652–3665.
- GARBET, X., SARAZIN, Y., BEYER, P., GHENDRIH, P., WALTZ, R., OTTAVIANI, M. & BENKADDA, S. 1999 Flux driven turbulence in tokamaks. *Nucl. Fusion* **39**, 2063–2068.
- GARBET, X., SARAZIN, Y., GHENDRIH, P., BENKADDA, S., BEYER, P., FIGARELLA, C. & VOITSEKHOVITCH, I. 2002 Turbulence simulations of transport barriers with toroidal velocity. *Phys. Plasmas* **9** (9), 3893–3905.
- GARBET, X., VARENNES, R., GILLOT, C., DIF-PRADALIER, G., SARAZIN, Y., BOURNE, E., GRANDGIRARD, V., GHENDRIH, P., ZARZOSO, D. & VERMARE, L. 2020 Zonal instability and wave trapping (in preparation).
- GILLOT, C. 2016 Study of the interaction between drift wave turbulence and zonal flows in a magnetic confinement device. Master’s thesis, Université Paris–Saclay.

- GILLOT, C. 2020 Model reduction for tokamak plasma turbulence: beyond fluid and quasi-linear descriptions. PhD thesis, Aix-Marseille Université.
- GIRARDO, J.-B. 2015 Control of instabilities and turbulence by fast particles in fusion plasmas. Theses, Ecode doctorale de l'Ecole Polytechnique (EDX).
- GIRARDO, J.-B., ZARZOSO, D., DUMONT, R., GARBET, X., SARAZIN, Y. & SHARAPOV, S. 2014 Relation between energetic and standard geodesic acoustic modes. *Phys. Plasmas* **21** (9), 092507.
- GÖRLER, T., LAPILLONNE, X., BRUNNER, S., DANNERT, T., JENKO, F., AGHDAM, S. K., MARCUS, P., MCMILLAN, B. F., MERZ, F., SAUTER, O., *et al.* 2011 Flux- and gradient-driven global gyrokinetic simulation of tokamak turbulence. *Phys. Plasmas* **18** (5), 056103.
- GÜRCAN, O. D., GARBET, X., HENNEQUIN, P., DIAMOND, P. H., CASATI, A. & FALCHETTO, G. 2009 Wave-number spectrum of drift-wave turbulence. *Phys. Rev. Lett.* **102** (25).
- HAGER, R. & HALLATSCHKEK, K. 2012 The nonlinear dispersion relation of geodesic acoustic modes. *Phys. Plasmas* **19** (8), 082315.
- HALLATSCHKEK, K. & BISKAMP, D. 2001 Transport control by coherent zonal flows in the core/edge transitional regime. *Phys. Rev. Lett.* **86** (7), 1223–1226.
- HASEGAWA, A. & MIMA, K. 1978 Pseudo-three-dimensional turbulence in magnetized nonuniform plasma. *Phys. Fluids* **21** (1), 87.
- HWA, T. & KARDAR, M. 1992 Avalanches, hydrodynamics, and discharge events in models of sandpiles. *Phys. Rev. A* **45** (10), 7002–7023.
- IDOMURA, Y., URANO, H., AIBA, N. & TOKUDA, S. 2009 Study of ion turbulent transport and profile formations using global gyrokinetic full-*f* Vlasov simulation. *Nucl. Fusion* **49** (6), 065029.
- IVANOV, P. G., SCHEKOCIHIN, A. A., DORLAND, W., FIELD, A. R. & PARRA, F. I. 2020 Zonally dominated dynamics and dimits threshold in curvature-driven ITG turbulence. *J. Plasma Phys.* **86** (5).
- JIMENEZ, J. & WHITHAM, G. B. 1976 An averaged Lagrangian method for dissipative wavetrains. *Proc. R. Soc. Lond. A* **349** (1658), 277–287.
- KAUFMAN, A. N., YE, H. & HUI, Y. 1987 Variational formulation of covariant eikonal theory for vector waves. *Phys. Lett. A* **120** (7), 327–330.
- KAW, P., SINGH, R. & DIAMOND, P. H. 2001 Coherent nonlinear structures of drift wave turbulence modulated by zonal flows. *Plasma Phys. Control. Fusion* **44** (1), 51–59.
- LANDAU, L. D. & LIFSCHITZ, E. M. 1984 *Electrodynamics of Continuous Media*. Pergamon.
- LAVAL, G., PESME, D. & ADAM, J.-C. 2018 Wave-particle and wave-wave interactions in hot plasmas: a French historical point of view. *Eur. Phys. J. H* **43** (4–5), 421–458.
- LIN, Z., ETHIER, S., HAHM, T. S. & TANG, W. M. 2002 Size scaling of turbulent transport in magnetically confined plasmas. *Phys. Rev. Lett.* **88** (19).
- MCDONALD, S. W. 1988 Phase-space representations of wave equations with applications to the eikonal approximation for short-wavelength waves. *Phys. Rep.* **158** (6), 337–416.
- MCDONALD, S. W. 1991 Wave kinetic equation in a fluctuating medium. *Phys. Rev. A* **43** (8), 4484–4499.
- MCDONALD, S. W. & KAUFMAN, A. N. 1985 Weyl representation for electromagnetic waves: the wave kinetic equation. *Phys. Rev. A* **32** (3), 1708–1713.
- MCMILLAN, B. F., HILL, P., BOTTINO, A., JOLLIET, S., VERNAY, T. & VILLARD, L. 2011 Interaction of large scale flow structures with gyrokinetic turbulence. *Phys. Plasmas* **18** (11), 112503.
- MCMILLAN, B. F., JOLLIET, S., TRAN, T. M., VILLARD, L., BOTTINO, A. & ANGELINO, P. 2009 Avalanchelike bursts in global gyrokinetic simulations. *Phys. Plasmas* **16** (2), 022310.
- MCMILLAN, B. F., PRINGLE, C. C. T. & TEACA, B. 2018 Simple advecting structures and the edge of chaos in subcritical tokamak plasmas. *J. Plasma Phys.* **84** (6).
- MOYAL, J. E. & BARTLETT, M. S. 1949 Quantum mechanics as a statistical theory. *Math. Proc. Cambridge* **45** (1), 99.
- NEWMAN, D. E., CARRERAS, B. A., DIAMOND, P. H. & HAHM, T. S. 1996 The dynamics of marginality and self-organized criticality as a paradigm for turbulent transport. *Phys. Plasmas* **3** (5), 1858–1866.
- PARKER, J. B. 2015 Zonal flows and turbulence in fluids and plasmas. PhD thesis, Princeton University.
- PARKER, J. B. 2016 Dynamics of zonal flows: failure of wave-kinetic theory, and new geometrical optics approximations. *J. Plasma Phys.* **82** (6).

- PRINGLE, C. C. T., MCMILLAN, B. F. & TEACA, B. 2017 A nonlinear approach to transition in subcritical plasmas with sheared flow. *Phys. Plasmas* **24** (12), 122307.
- QIU, Z., CHEN, L. & ZONCA, F. 2018 Kinetic theory of geodesic acoustic modes in toroidal plasmas: a brief review. *Plasma Sci. Technol.* **20** (9), 094004.
- RATH, F., PEETERS, A. G., BUCHHOLZ, R., GROSSHAUSER, S. R., MIGLIANO, P., WEIKL, A. & STRINTZI, D. 2016 Comparison of gradient and flux driven gyro-kinetic turbulent transport. *Phys. Plasmas* **23** (5), 052309.
- RUIZ, D. E. 2017 A geometric theory of waves and its applications to plasma physics. PhD thesis, Princeton University.
- RUIZ, D. E., GLINSKY, M. E. & DODIN, I. Y. 2019 Wave kinetic equation for inhomogeneous drift-wave turbulence beyond the quasilinear approximation. *J. Plasma Phys.* **85** (1).
- RUIZ, D. E., PARKER, J. B., SHI, E. L. & DODIN, I. Y. 2016 Zonal-flow dynamics from a phase-space perspective. *Phys. Plasmas* **23** (12), 122304.
- SARAZIN, Y. & GHENDRIH, P. 1998 Intermittent particle transport in two-dimensional edge turbulence. *Phys. Plasmas* **5** (12), 4214–4228.
- SARAZIN, Y., GRANDGIRARD, V., ABITEBOUL, J., ALLFREY, S., GARBET, X., GHENDRIH, P., LATU, G., STRUGAREK, A. & DIF-PRADALIER, G. 2010 Large scale dynamics in flux driven gyrokinetic turbulence. *Nucl. Fusion* **50** (5), 054004.
- SASAKI, M. 2018 Trapping of turbulence clumps by geodesic acoustic modes. In *AIP Conference Proceedings 1993*, 020007.
- SASAKI, M., ITOH, K., KOBAYASHI, T., KASUYA, N., FUJISAWA, A. & ITOH, S.-I. 2018a Propagation direction of geodesic acoustic modes driven by drift wave turbulence. *Nucl. Fusion* **58** (11), 112005.
- SASAKI, M., KASUYA, N., ITOH, K., HALLATSCHEK, K., LESUR, M., KOSUGA, Y. & ITOH, S.-I. 2016 A branch of energetic-particle driven geodesic acoustic modes due to magnetic drift resonance. *Phys. Plasmas* **23** (10), 102501.
- SASAKI, M., KOBAYASHI, T., ITOH, K., KASUYA, N., KOSUGA, Y., FUJISAWA, A. & ITOH, S.-I. 2018b Spatio-temporal dynamics of turbulence trapped in geodesic acoustic modes. *Phys. Plasmas* **25** (1), 012316.
- SCHEKOCIHIN, A. A., HIGHCOCK, E. G. & COWLEY, S. C. 2012 Subcritical fluctuations and suppression of turbulence in differentially rotating gyrokinetic plasmas. *Plasma Phys. Control. Fusion* **54** (5), 055011.
- SCOTT, B. & SMIRNOV, J. 2010 Energetic consistency and momentum conservation in the gyrokinetic description of tokamak plasmas. *Phys. Plasmas* **17** (11), 112302.
- SRINIVASAN, K. & YOUNG, W. R. 2012 Zonostrophic instability. *J. Atmos. Sci.* **69** (5), 1633–1656.
- STAEBLER, G. M., WALTZ, R. E., CANDY, J. & KINSEY, J. E. 2013 New paradigm for suppression of gyrokinetic turbulence by velocity shear. *Phys. Rev. Lett.* **110**, 055003.
- SUCHY, K. 1981 Real Hamilton equations of geometric optics for media with moderate absorption. *Radio Sci.* **16** (6), 1179–1182.
- TAYLOR, G. I. 1915 I. Eddy motion in the atmosphere. *Phil. Trans. R. Soc. Lond. A* **215** (523–537), 1–26.
- VILLARD, L., MCMILLAN, B. F., LANTI, E., OHANA, N., BOTTINO, A., BIANCALANI, A., NOVIKAU, I., BRUNNER, S., SAUTER, O., TRONKO, N., *et al.* 2019 Global turbulence features across marginality and non-local pedestal-core interactions. *Plasma Phys. Control. Fusion* **61** (3), 034003.
- WALTZ, R. E. & HOLLAND, C. 2008 Numerical experiments on the drift wave–zonal flow paradigm for nonlinear saturation. *Phys. Plasmas* **15** (12), 122503.
- WEINBERG, S. 1962 Eikonal method in magnetohydrodynamics. *Phys. Rev.* **126** (6), 1899–1909.
- WHITHAM, G. B. 1965 A general approach to linear and non-linear dispersive waves using a Lagrangian. *J. Fluid Mech.* **22** (2), 273–283.
- VAN WYK, F., HIGHCOCK, E. G., SCHEKOCIHIN, A. A., ROACH, C. M., FIELD, A. R. & DORLAND, W. 2016 Transition to subcritical turbulence in a tokamak plasma. *J. Plasma Phys.* **82** (6).
- ZARZOSO, D., SARAZIN, Y., GARBET, X., DUMONT, R., STRUGAREK, A., ABITEBOUL, J., CARTIER-MICHAUD, T., DIF-PRADALIER, G., GHENDRIH, P., GRANDGIRARD, V., *et al.* 2013 Impact of energetic-particle-driven geodesic acoustic modes on turbulence. *Phys. Rev. Lett.* **110** (12).

- ZHU, H., ZHOU, Y. & DODIN, I. Y. 2018*a* On the structure of the Drifton phase space and its relation to the Rayleigh–Kuo criterion of the zonal-flow stability. *Phys. Plasmas* **25** (7), 072121.
- ZHU, H., ZHOU, Y. & DODIN, I. Y. 2020 Theory of the tertiary instability and the limits shift from reduced drift-wave models. *Phys. Rev. Lett.* **124** (5).
- ZHU, H., ZHOU, Y., RUIZ, D. E. & DODIN, I. Y. 2018*b* Wave kinetics of drift-wave turbulence and zonal flows beyond the ray approximation. *Phys. Rev. E* **97** (5).